ELSEVIER

Electrical Power and Energy Systems 25 (2003) 581–589

ELECTRICAL POWER & ENERGY SYSTEMS

www.elsevier.com/locate/ijepes

Modeling secondary arc based on identification of arc parameters from staged fault test records

László Prikler[a,*], Mustafa Kizilcay[b], Gábor Bán[a], Péter Handl[a]

[a]*Department of Electric Power Engineering, Budapest University of Technology and Economics, Egry J. 18, H-1111 Budapest, Hungary*
[b]*Department of Electrical Engineering and Computer Science, Osnabrück University of Applied Sciences, Albrechtstr. 30, D-49076 Osnabrück, Germany*

Abstract

A realistic representation of the secondary arcs is essential in determining the auto-reclosure performance of EHV transmission lines. In this paper the dynamic behavior of the arc is presented as a time-varying resistance using the MODELS feature of the ATP–EMTP program. It is shown that random variation of the arc parameters influences significantly the arc extinction time besides the capacitive and inductive coupling between the faulty and the sound phases. Parameters for the arc model have been extracted from staged fault tests records carried out on a double-circuit, uncompensated 400 kV interconnecting line. The results of the simulation proved the importance of the distributed nature of the transmission line and the nonlinear characteristic of the arc resistance in the intermittent region of arcing. The arc current is determined by wave processes in this interval. As a result, the continuous current characterizing the first period of secondary arcing is followed by individual current impulses of much higher amplitude. The high energy re-ignitions of the second period may push back the arcing process into the continuous condition, which multiplies the self-extinction time.

Keywords: Line fault; Secondary arc; Simulation identification; Measurement; EMTP–ATP

1. Introduction

Faults on solidly grounded EHV/UHV transmission lines are single-phase-to-ground ones and not permanent in the majority of cases, thus *single-phase auto-reclosure* (SPAR) eliminates the predominant part of the faults. The successfulness of the reclosure is, however, endangered by *long duration secondary arcing* [1,2].

The secondary arc follows the heavy current fault arc in the ionized, hot plasma channel after isolating the fault by single-pole tripping in an EHV transmission line. It is sustained by the capacitive and inductive coupling to the sound phase-conductors. The secondary arc self-extinguishes usually, but its life-time may have a strong influence to the reliability of the operation of the line: on the one hand a non-self-extinguishing secondary arc endangers the efficiency of the single-phase reclosing; on the other hand prolonging the dead time (switched-off interval of the faulty phase) is limited by dynamic stability constraints. This limit is usually less than 1.5–2 s for a long EHV/UHV interconnection. In particular for compact lines with reduced clearances the smaller phase-to-phase clearances make the capacitive coupling between conductors more substantial, which may result in higher secondary arc currents and longer arcing times.

2. Increasing importance of SPAR successfulness

Public expectations require radical integration of the power system components into the environment. As a consequence, to find a new right-of-way is rather difficult. Using compact tower construction and upgrading existing lines offer a possibility to overcome these constraints. However, reducing the phase-to-phase clearances has a strong impact on the lightning and switching performance of the line. It can be expected that the number of faults will increase drastically, which contradicts another key expectation of the public today: the *quality of supply*.

Auto-reclosure is an efficient tool to compensate the expected growth in the number of line faults. This condition emphasizes the importance of studying the ways of increasing the SPAR effectiveness. Namely, improving the SPAR efficiency could compensate the increase in the number of faults caused by lightning strokes which is presumable in any compact line design because of the reduced insulation distances [3–6]. The successfulness of

* Corresponding author. Tel.: +36-1-463-3015; fax: +36-1-463-3013.
E-mail address: prikler@vmt.bme.hu (L. Prikler); kizilcay@fhos.de (M. Kizilcay)

0142-0615/03/$ - see front matter © 2003 Elsevier Science Ltd. All rights reserved.
doi:10.1016/S0142-0615(03)00018-8

SPAR is endangered by:

(a) *Long duration secondary arcs*. The secondary arc extinguishes spontaneously as a rule, however, its duration depends on many factors, mainly on the value of the secondary arc current.
(b) *Reclosing overvoltages* can re-ignite the arc at the place of the fault. The reclosing transients may result in high overvoltages at the receiving end of the line, especially when trapped charge occurs on the phase conductor before the reclosure.

2.1. Single-phase reclosing is problematic at compact line configurations

The application of SPAR is more problematic for compact lines of reduced dimensions. When neglecting other influencing factors, the bigger the phase-to-phase capacitance (C_{ab}), the higher the secondary arc current and the longer the secondary arcing duration. Both compacting and upgrading power lines may result in increasing C_{ab}, i.e. longer secondary arc duration.

Table 1 shows that a compact or upgraded line has a double or higher C_{ab} in comparison with a conventional one. Considering the increase of the rate of rise of the secondary arc duration as a function of the arc current, it can be expected that unacceptable long extinction times would occur in compact transmission line configurations.

3. The necessity of secondary arc model for computer simulations

It is nearly impossible to reproduce the real arc behavior by computer simulation due to the extremely random character of the arc. This process reflects a peculiar interaction of the line and the arc. For this reason the simulation has to consider the functions describing the impulse arc characteristics, the recovery of the insulation following the partial extinctions as well, beside the electromagnetic transients.

Any arc model requires several input parameters which could be obtained by measurements only. Parameters extracted from measurements can be used to elaborate an arc model which reproduces quite well the main characteristics of that specific arc measurement [7–9]. Such a model might give less reliable results for other arcing conditions on the same line, or completely inaccurate results for experiments carried out on other lines with different length, voltage level and conductor arrangement.

However, a computer simulation of the process leading to the secondary arc extinction can be a suitable tool for *sensitivity studies* to identify the main influencing factors and to find the *similitude invariants*, which are necessary to compile generalized diagrams for the estimation of the arcing time.

Table 1
Positive, zero and mutual capacitance of typical conventional and compact 400 kV lines

Line configuration	C_0 (nF/km)	C_1 (nF/km)	C_{ab} (nF/km)
Conventional 400 kV	8.235	10.958	0.907
Compact 400 kV line (2×500 mm^2 phase conductors)	7.03	12.55	1.83
Compact 400 kV line (3×300 mm^2 phase conductors)	7.46	13.95	2.16

4. Existing arc models

In simplified digital studies, the fault arc is very often represented by a resistor or as a voltage source with periodic rectangular wave changing its sign at each zero crossing of the arc current. More sophisticated models describe the arc by piecewise characteristics. These models do *not* take into account the real interaction of the arc and the electromagnetic transient on the line during the arcing process correctly, since sudden changes in the arcing conditions arise following a partial arc extinction.

Existing secondary arc models are based on the differential equation of the arc conductance which describes the energy balance of the arc column

$$\frac{\mathrm{d}g}{\mathrm{d}t} = \frac{1}{\tau}(G - g) \tag{1}$$

where

τ is the time constant of the arc,
g is the instantaneous arc conductance,
G is the stationary arc conductance.

The stationary arc conductance can be defined as

$$G = \frac{|i_{\mathrm{arc}}|}{(u_0 + r_0|i_{\mathrm{arc}}|)l_{\mathrm{arc}}(t)} \tag{2}$$

where

l_{arc} is the instantaneous arc length,
u_0 is the characteristic arc voltage,
r_0 is the characteristic arc resistance per arc length.

Parameters τ, u_0, r_0 can be obtained from measurements as will be shown in Section 7. The time constant of the arc is inversely proportional to the arc length and can be defined by the following expression

$$\tau(l) = \tau_0\left(\frac{l_{\mathrm{arc}}}{l_0}\right)^{\alpha} \tag{3}$$

where

τ_0 is the initial time constant,
l_0 is the initial arc length,
α is the coefficient in a range: -0.1 to -0.6.

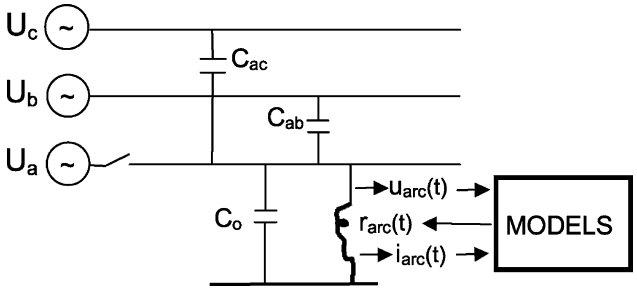

Fig. 1. Interaction between the electrical circuit and the arc model.

The time-dependent arc elongation $l_{arc}(t)$ is the most significant factor which influences the arc extinction and arcing duration. Since the length variation of the secondary arc is highly dependent on environmental impacts like wind and thermal buoyancy, it is difficult to consider these random effects accurately in the numerical model. Nevertheless the above arc model can be used successfully to estimate the maximum arcing duration as worst case or to understand the interaction of the secondary arc with the electrical circuit.

Refs. [10,11] point out that models based on the differential equation of the arc conductance can be applied for modeling high current primary arcs. The secondary arc representation needs, however, further improvement because Eq. (1) considers only the *thermal re-ignition* of the arc and the subsequent *dielectric restrikes* are not taken into account.

5. Representation of the electrical arc in ATP–EMTP using models

The arc can be represented by a Type-91 TACS/MODELS controlled resistance in the Electromagnetic Transients Program, ATP–EMTP [12]. When solving the differential equation (1) in the s domain by using MODELS's [13] LAPLACE function, the time varying arc conductance g can be obtained as:

$$g(t) = \frac{1}{1+\tau s} G(t) \tag{4}$$

The elongation of the arc can be considered when updating $G(t)$, using the arc current from the previous time step. Time constant τ is itself a function of the arc length, that can be considered when solving Eq. (4). The calculated $r_{arc}(t) = 1/g(t)$ will become active in the next time step in the electrical circuit as shown in Fig. 1.

6. Experimental data about secondary arc extinction times

Numerous tests have been carried out in real lines and laboratories to get a reliable picture about the secondary arc duration. The secondary arcing times recorded on real lines and laboratory tests, and published in technical papers [1, 14] show a significant spread. This spread can be explained by the extremely random character of the arc formation and the strong influence of many parameters (wind velocity, the movement of the hot plasma generated by the primary arc, magnetic force due to the current, convection of the plasma and surrounding air, presence and degree of shunt compensation with four- or three-legged reactor sets, etc.) to the arcing time.

6.1. Staged fault tests on a 400 kV double-circuit line

Authors participated in field testing of a double circuit, 400 kV interconnecting line of 230 km length, without shunt compensation. The line has been operated by connecting the two circuits in parallel along the 1/3rd of the full length in the first test case. The remaining sections of the 2nd circuit have been disconnected from the tested line or were grounded.

Seven staged faults have been carried out, aiming to predict the secondary arcing times. The arc has been initiated by a thin grounding wire connected to one of the isolated phases to omit the primary arc. This arc ignition technique is

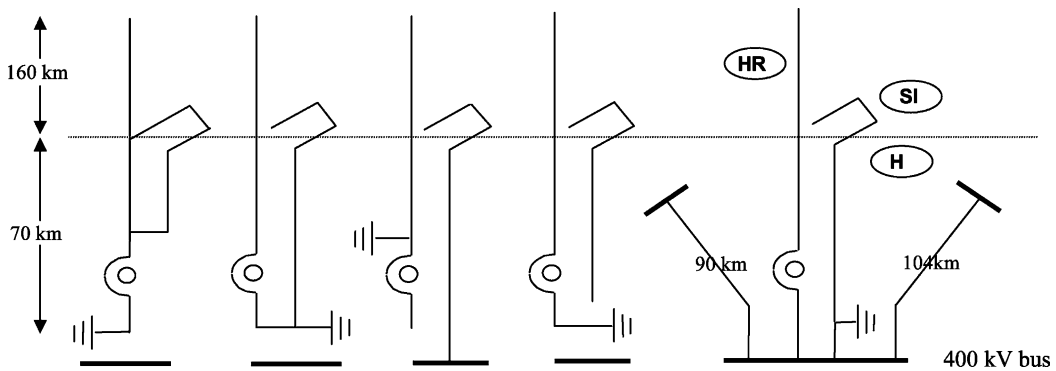

Fig. 2. Measuring arrangements at staged fault tests: no primary arc in case 1–4, with primary arc in case 5 (rightmost).

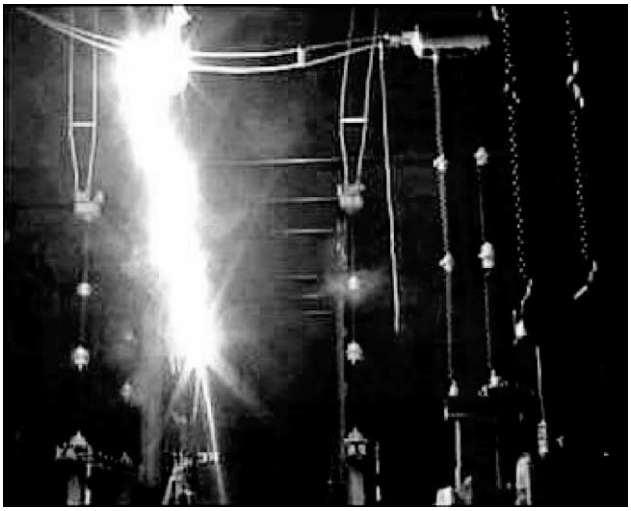

Fig. 3. Permanent 400 kV secondary arc at calmness.

able to provide comparable results to the tests with primary arcs if the expected secondary arcing time exceeds 700 ms [14]. The plasma cloud of the primary arc moves upward with a given speed, thus it certainly has a strong influence to the shorter secondary arcs, but such a self-extinguishing short arc does not endanger the SPAR successfulness.

The measuring arrangement and the length of the faulty phases are shown in Fig. 2. The location of the staged fault is indicated by a grounding symbol. The arc current (or part of it) has been measured by service CTs.

6.2. Test results

The shortest extinction time recorded during the tests was 0.05 s and the longest one was 4 s. The secondary arc did not extinguish during 27 s at one of the tests. Extinction times of 4 and 27 s have been measured at calmness. As Fig. 3 shows, at calmness the secondary arc has not any significant horizontal component and as a consequence no relevant channel elongation is seen. Ions generated during the intermittent arc interval remain in the environment of the arc. These circumstances make the self-extinction time very long.

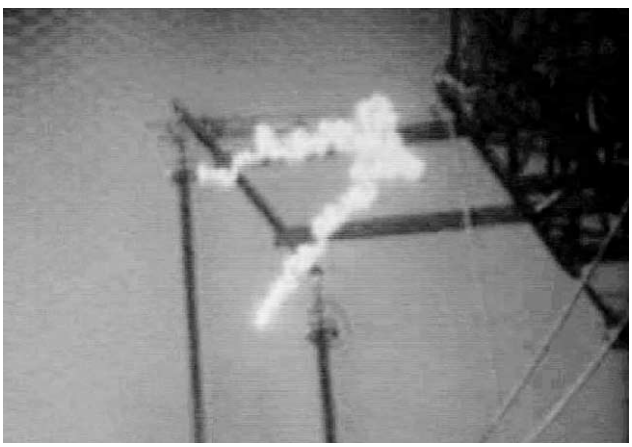

Fig. 4. Secondary arc in middle velocity (3–4 m/s) wind along a 400 kV non-ceramic insulator.

The secondary arcing times recorded at moderate (3–4 m/s) wind velocities were 0.05–0.69 s. As Fig. 4 shows the elongation of the arc is slow. Due to the electromagnetic field, loops occur in the arc channel.

The big spread of the extinction times and very long arcing times experienced in two cases correspond to the data about extinction times published in former papers containing generalized diagrams [1].

7. Arc parameter determination

Secondary arc parameters u_0 and τ could be obtained only in certain time intervals due to required high accuracy of measured arc current and voltage. The parameters u_0 and τ are determined by numerical integration in each half period assuming their values remain unchanged in a half period

$$u_0 = \frac{\int_{t_1}^{t_2} |i_{\text{arc}}| \mathrm{d}t}{\int_{t_1}^{t_2} g \, \mathrm{d}t} \tag{5}$$

$$\tau = \frac{\frac{1}{u_0}\int_{t_1}^{t_3} |i_{\text{arc}}| \mathrm{d}t - \int_{t_1}^{t_3} g \, \mathrm{d}t}{g(t_3) - g(t_1)} \tag{6}$$

where

$g = i/u$ is the instantaneous arc conductance,
t_1 and t_2 are time points, where $g(t_1) = g(t_2)$,
t_3 is the time point within a half period, where g becomes maximum.

Fig. 5 shows the secondary arc parameters identified in the time interval (0.63–0.74 s), as an example.

8. Final extinction of the secondary arc

The most challenging task of arc modeling is to specify conditions leading to the final arc extinction. Some of the models determine arc extinction according to time derivative of the instantaneous arc resistance: if derivative is higher and the instantaneous conductance is lower than a limit, the secondary arc extinguishes. Other models, like the one presented in Ref. [10], proposes extinction criteria of a dielectric type: the arc extinguishes at each current reversal, and the arc conductance is kept zero as long as the recovery voltage is below a limit obtained by an empirical formula.

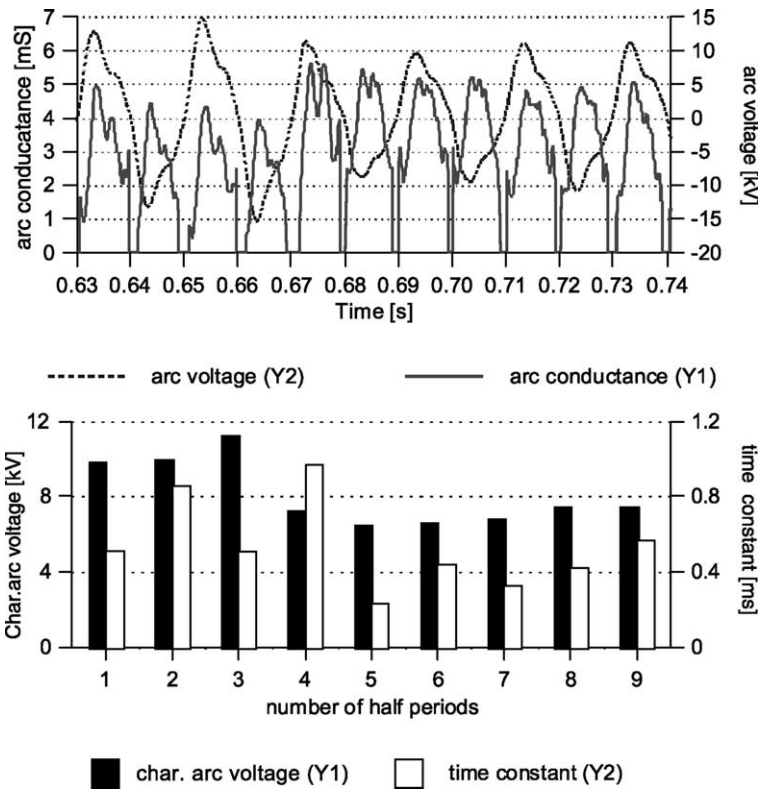

Fig. 5. Secondary arc parameters u_0 and τ obtained from measurement.

8.1. Processes leading to the arc extinction

The main condition of the spontaneous extinction of the secondary arc is a strong air movement, which makes the arc to elongate quickly. The hot plasma generated by the primary arc moves upward with a high velocity, resulting in an initial vertical component for the secondary arc elongation (Fig. 6). Wind has the same effect on the secondary arc. The speedy elongation of the arc produces high conductance plasma clouds separated from each other by high resistance channel zones. So the resistance of the whole arc length increases and the amplitude of the sinusoidal current decreases. The recovery voltage at the faulty place makes the high resistance arc channel zones re-ignite during the arc elongation process. As a consequence the secondary current stops to be sinusoidal.

When the number of high resistance zones increases, the amplitude of the operating frequency current component decreases and high amplitude impulses occur as a consequence of growing the re-ignition voltage. If

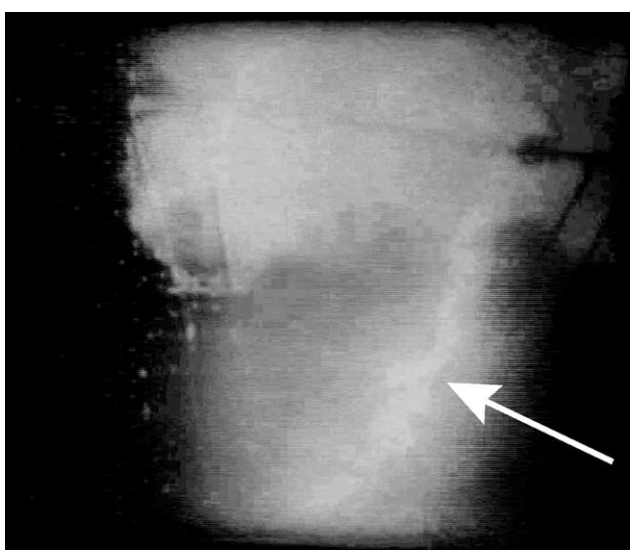

Fig. 6. Formation of the secondary arc inside the plasma cloud of the primary arc.

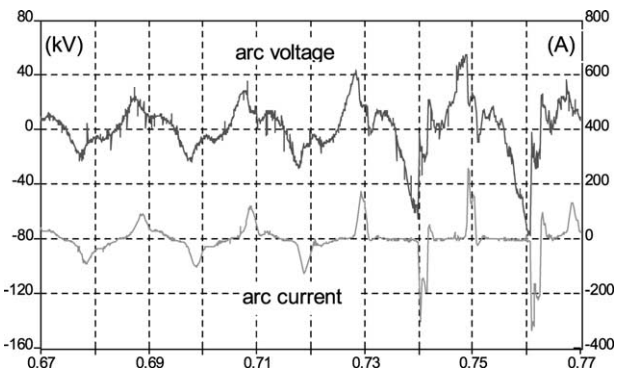

Fig. 7. Measured secondary arc voltage and current.

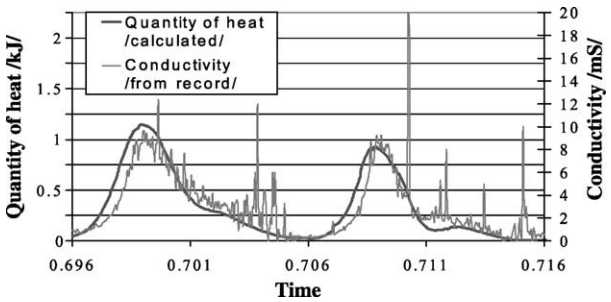

Fig. 8. Energy content and conductivity of the arc.

the recovery voltage is sufficient to produce a breakdown, bridging a significant length of the arc channel, the arcing process may return to the steady-state condition, remarkably prolonging the self-extinction time. The secondary arc extinguishes finally, if the re-ignition voltage exceeds the amplitude of the recovery voltage.

As the curves of Fig. 7 reflect, the final extinction of the secondary arc is always preceded by an intermittent interval, when high current impulses are superimposed on the low amplitude operating frequency component of the current. The amplitude of these impulses is much higher than the peak value of the steady-state current.

The sudden re-ignitions in the arc channel initiate wave phenomena on the line. The superposition of the reflected waves produces a current zero in the arc channel resulting in a partial arc extinction. The length of the current impulses depends on the place of the fault. For the predominant part of the line length, the duration of these impulses is twice of the line travel time.

The energy of the current impulse is higher, when the re-ignition occurs near to, but before the peak of the recovery voltage. The high current impulse is able to re-ionize a large amount of plasma, resulting a fallback into the quasi-sinusoidal phase of the arcing process which elongates the secondary arc duration. As an example, the energy and the conductivity of the arc channel are plotted in Fig. 8.

The quantity of the heat has been obtained from Eq. (7), the conductivity is derived from measurements of Fig. 7

$$Q_i = t_{\text{sample}} \sum_{j=0}^{j=N} (U_{i-j} I_{i-j}) \mathrm{e}^{-jt_{\text{sample}}/\tau} \tag{7}$$

where

t_{sample} is the sampling time = 0.05 ms,
τ is the time constant of the arc.

8.2. Dielectric strength of the secondary arc channel

At constant air pressure the electrical field strength of the arc channel can be obtained by the following formula [15]

$$E(t) = E_\infty \frac{T_\infty}{(T_0 - T_\infty)\mathrm{e}^{-t/\tau} + T_\infty} \approx E_\infty \frac{T_\infty}{T_0} \mathrm{e}^{t/\tau} \tag{8}$$

where

τ is the time constant of the arc,
T_∞ is the ambient temperature,
T_0 is the temperature of the arc channel at current zero,
E_∞ is the field strength at temperature T_∞.

The final extinction of the secondary arc is bound up with the regeneration rate which depends on the actual temperature of the arc channel. If the time constant τ is

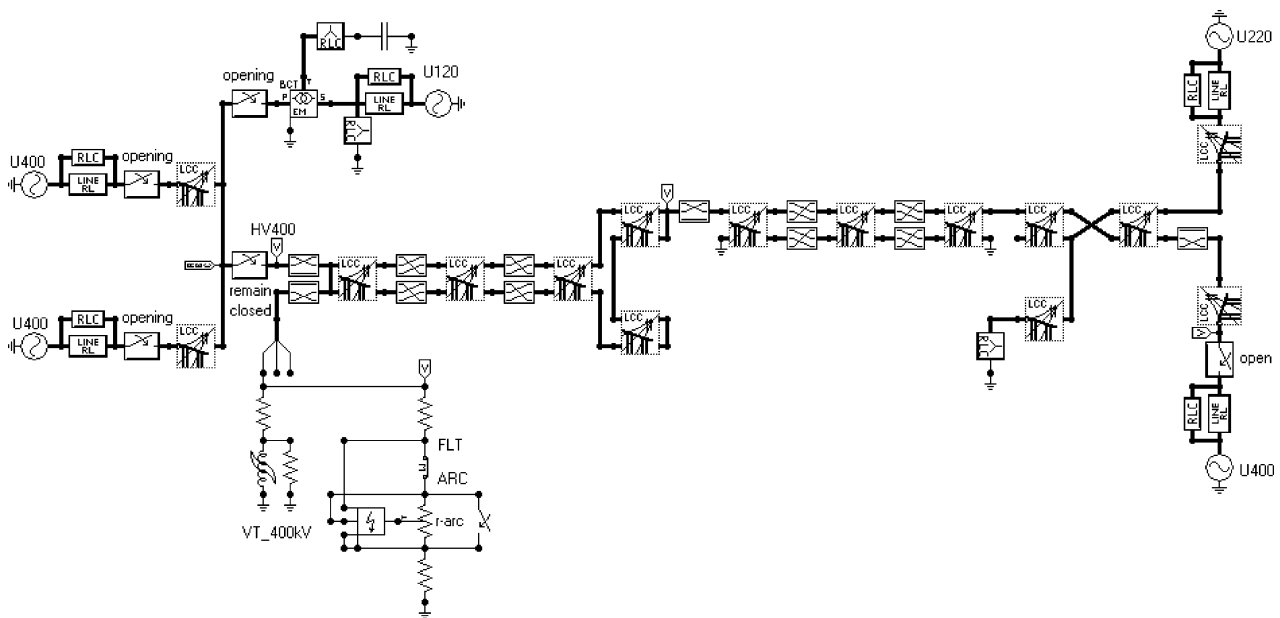

Fig. 9. ATPDraw circuit of the tested 400 kV interconnection. The arc model is connected to phase A of bus HV400.

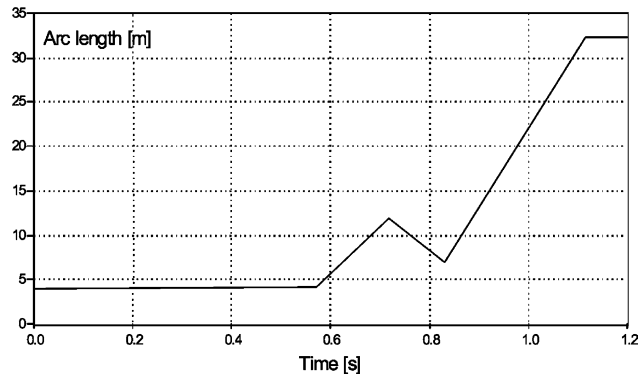

Fig. 10. Arc elongation during the arcing process.

large, the arc will finally extinguish just after a relatively long time (or it may not extinguish in extreme cases) because the high arc temperature increases the probability of a dielectric restrike.

9. ATP–EMTP model of the tested 400 kV interconnection

The ATP–EMTP model of the test arrangement in Section 6 has been assembled by using the ATPDraw graphical preprocessor [16]. The model shown in Fig. 9 corresponds to the rightmost measuring arrangement of Fig. 2 and has been elaborated to prove the main characteristics of the recorded arc currents and voltages.

The arc model which was written in MODELS simulation language has been connected to the circuit at node HV400. Following arc parameters have been used at the simulation:

$$u_0 = 0.9\ \text{kV/m},\ \tau_0 = 1\ \text{ms},\ r_0 = 22\ \text{m}\Omega\text{/m},\ \alpha = -0.5.$$

The time-varying arc elongation, $l_{\text{arc}}(t)$ has been derived by inspection of measured arc voltage and is given in Fig. 10.

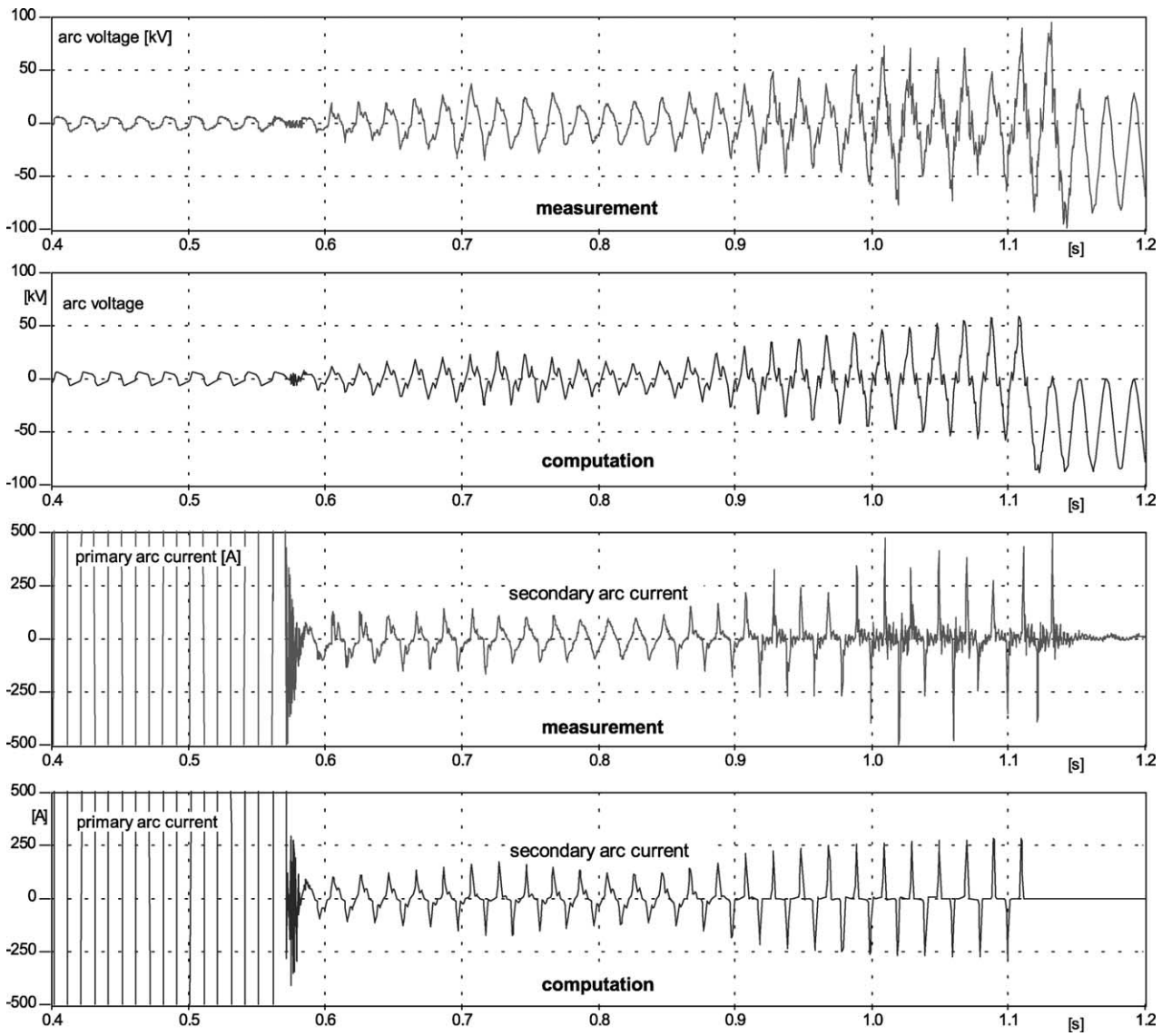

Fig. 11. Measured and computed arc voltages and current.

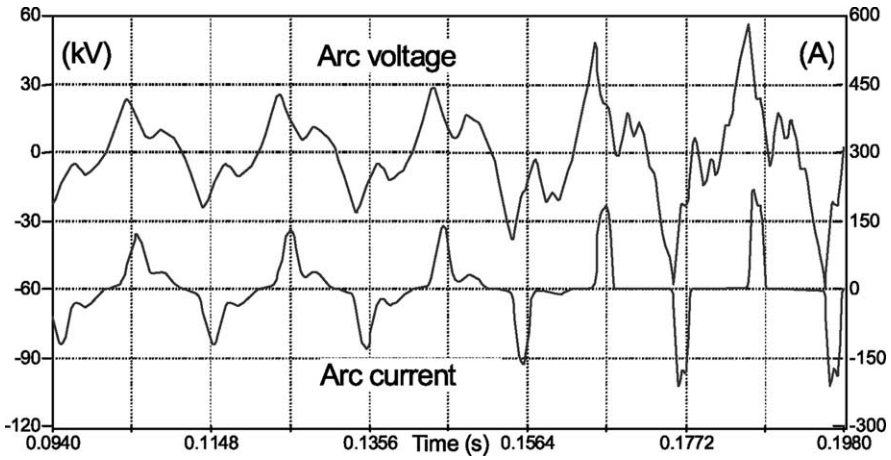

Fig. 12. Simulated secondary arc voltage and current.

Limiting values per arc length for arc extinction were:

$$g'_{\min} = 50\ \mu\text{S m}, \qquad \frac{\mathrm{d}r'_{\text{arc}}}{\mathrm{d}t} = 20\ \text{M}\Omega/(\text{s m}) \tag{9}$$

The arc extinguishes, if the time derivative of instantaneous arc resistance, $\mathrm{d}r_{\text{arc}}/\mathrm{d}t$, exceeds the above limit provided arc conductance g per length is less than $g'_{\min}$. This criterion considers only the thermal extinction of the arc. Possible subsequent dielectric re-ignitions in air were not taken into account. Fig. 11 shows the measured and computed arc voltages and currents, respectively.

The high current primary arc passes into secondary arcing when the 'remote' circuit breakers in the system shown in Fig. 9 cleared the fault at $t = 0.57$ s. The arc simulation results are in good agreement with the measured arc voltages and currents.

Fig. 12 shows the simulated arc voltage and current of a permanent secondary arc (Figs. 3 and 7) during an intermittent interval. The high current peaks of rectangular shape are produced by re-ignitions close to peak value of the recovery voltage. As Fig. 12 shows, the power frequency component of the arc current has minor importance at the partial extinction period.

10. Conclusions

- Improving the efficiency of reclosing could compensate the increase in the number of faults caused by lightning strokes which is desirable in any compact or upgraded lines because of the reduced insulation distances.
- The results of secondary arc field tests spread to a great extent due to the differences in the wind velocities, arc initiation technique, line construction, shunt compensation degree, etc. Recording the wind velocity in the environment of the secondary arc and a detailed description of the way of arc initiation would reduce the spread of the experimental data.
- Due to the highly random and complex behavior of the secondary arc it is very difficult to reproduce the exact arc duration by digital simulations. However, the models elaborated in this paper can be employed successfully to examine the performance of arc suppression schemes in auto-reclosure studies.
- Computer simulation is a suitable tool for sensitivity studies to find main factors influencing the secondary arcing process and to find the similitude invariants which are necessary to compile generalized diagrams.
- Secondary arc parameters can be extracted from field test records by numerical integration of arc currents and voltages. However, service transducers' accuracy is generally not sufficient for such kind of measurements.
- The extinction time of the secondary arc is affected by the shape and amplitude of the recovery voltage arising after each transient current zero at the place of the fault.
- The final extinction of the secondary arc is bound up with the regeneration rate of the arc channel. The high arc temperature increases the probability of a dielectric restrike and the extinction time is proportional with the time constant of the arc.
- Test circuits used in many HV laboratories to predict the secondary arc extinction times consist of lumped elements only, thus wave processes on the line during the partial extinction period of arcing cannot be considered.
- Systematic laboratory tests at which the wind velocity can be controlled and all parameters are correctly recorded can provide reliable data if the transients of intermittent arcing are well simulated. Using correct laboratory test circuits, the validity of tests without primary arc and the suitable technique of arc ignition could be investigated exactly. This is a way to improve the reliability of the field test results.

Acknowledgements

The activity reported in this paper has been partly supported by the Hungarian Research Fund under contract OTKA T-035178. Authors acknowledge the contribution of the Hungarian Power Companies Ltd to the field measurements.

References

[1] Haubrich HJ, Hosemann G, Thomas R. Single-phase auto-reclosing in EHV systems. CIGRE 1974; Rep. 31-09.
[2] IEEE. Single-phase tripping and auto reclosing of transmission lines. IEEE Trans Power Delivery 1992;7(1):182–92
[3] Prikler L, Bán G, Bánfai G, Handl P. Testing and simulation of EHV secondary arcs. Proceedings of the European EMTP–ATP Conference, Bristol, UK; September 3–5 2001.
[4] Bán G. Single-phase reclosing EHV transmission lines. Proceedings of the 17th Hungarian–Korean Seminar, EHV Technologies-II, Keszthely-Lake Balaton, Hungary; October 2001.
[5] Bán G, Prikler L, Bánfai G. Testing, EHV, secondary arcs. IEEE Porto Power Tech'01 Conference, Porto, Portugal; September 9–13 2001.
[6] Bán G, Prikler L, Bánfai G. The use of neutral reactors for improving the successfulness of 3-phase reclosing. IEEE Budapest Power Tech'99 Conference, Budapest, Hungary; August 29–September 2 1999.
[7] Kizilcay M, Pniok T. Digital simulation of fault arcs in power systems. ETEP J 1991;1(1):55–60.
[8] Kizilcay M, Koch K.-H. Numerical fault arc simulation based on power arc tests. ETEP J 1994;4(3):177–86.
[9] Terzija VV, Wehrmann S. Long arc in still air: testing, modelling and simulation. EEUG News 2001;7(3):44–54.
[10] Johns AT, Aggarwal RK, Song YH. Improved techniques for modeling fault arcs on faulted EHV transmission system. Proc IEE—Gener, Transm Distrib 1994;141(2):148–54.
[11] Kizilcay M. Evaluation of existing secondary arc models. EEUG News 1997;3(2):49–60.
[12] Alternative Transient Program Rule Book, Can/Am EMTP User Group, USA; 1997.
[13] Dubé L. Models in ATP. Language manual; 1996. http://www.eeug.org/files/secret/models.
[14] Rashkes VS. Generalization of the operation experiences, connected with the efficiency of single-phase reclosing, experimental data about the extinction time of the secondary arc. Elektricheskie Stancii 1989; 3. (in Russian).
[15] Danyek M, Handl P. Improving the reliability of experimental data about secondary arc duration. Proceedings of the 17th Hungarian–Korean Seminar, EHV Technologies-II, Keszthely-Lake Balaton, Hungary; October 2001.
[16] Prikler L, Høidalen HK. ATPDraw version 3.5 for Windows9x/NT/2000/XP-User's Manual, SINTEF Energy Research AS, Norway, TR F5680, ISBN 82-594-2344-8; August 2002.